

Article

Influence of Shaped Hole and Seed Disturbance on the Precision of Bunch Planting with the Double-Hole Rice Vacuum Seed Meter

Cheng Qian ^{1,2} , Siyu He ^{1,2}, Wei Qin ^{1,2}, Youcong Jiang ^{1,2}, Zishun Huang ^{1,2}, Meilin Zhang ^{1,2}, Minghua Zhang ^{1,2,3,4,5}, Wenwu Yang ^{1,2,3,4,5,*} and Ying Zang ^{1,2,3,4,5,*}

- ¹ Guangdong Laboratory for Lingnan Modern Agriculture, College of Engineering, South China Agricultural University, Guangzhou 510642, China; chengqian@stu.scau.edu.cn (C.Q.); heside9527@scau.edu.cn (S.H.); qinweilxy@scau.edu.cn (W.Q.); jiangyc@stu.scau.edu.cn (Y.J.); huangzs@stu.scau.edu.cn (Z.H.); mlzhang@stu.scau.edu.cn (M.Z.); zhangminghuascau@163.com (M.Z.)
- ² Key Laboratory of Key Technology on Agricultural Machine and Equipment, Ministry of Education, South China Agricultural University, Guangzhou 510642, China
- ³ Guangdong Provincial Key Laboratory of Agricultural Artificial Intelligence (GDKL-AAI), Guangzhou 510642, China
- ⁴ Maoming Branch, Guangdong Laboratory for Modern Agriculture, Maoming 525000, China
- ⁵ Huangpu Institute of Innovation, College of Engineering, South China Agricultural University, Guangzhou 510642, China
- * Correspondence: yangwenwu@scau.edu.cn (W.Y.); yingzang@scau.edu.cn (Y.Z.)

Abstract: The double-hole rice vacuum seed meter is critical equipment for the planting precision of rice direct seeding. The effects of shaped holes and seed disturbance on the precision of rice bunch planting were investigated to improve the precision of bunch planting with the double-hole rice vacuum seed meter. A test bench with the rice vacuum seed meter was set up to analyze the trends in the quality of feed index, miss index, and multiple index of seed meters with different shaped holes at different speeds and vacuum pressures. Based on the optimal hole structure, different seed disturbance structures were designed to investigate the influence of the seed disturbance structure on the precision of bunch planting. A multiple linear regression model was established for the relationship between the disturbance structure, vacuum pressure, rotational speed, and the precision of bunch planting. Discrete element numerical simulation experiments were carried out to analyze the effect of disturbance structures on seeds. The planting precision of the seed meter with the shaped hole was significantly higher than that of the seed meter without the shaped hole while the shaped hole B was the optimum structure. Disturbance structure affects the quality of feed index, multiple index rate, and miss index. The planting precision of the seed disturbance structure II was better than the other structures. At a speed of 60 rpm and vacuum pressures of 2.0 kPa, 2.4 kPa, and 2.8 kPa, the qualities of feed index of seed disturbance structure II were 90%, 91.11%, and 89.17%, respectively, and the miss indexes were 2.96%, 1.94%, and 1.57%, respectively. At high rotational speeds, the precision of rice bunch planting with the seed disturbance structure is better than that without the seed disturbance structure. In the simulation test, the seed velocity and total force magnitude of the meter without disturbance structures were less than those with the disturbed structure. Simulation experiments showed that the seed disturbance structure breaks up the stacked state of seeds. Research has shown that the shaped hole holds the seed in a stable suction posture, which helps to increase the seed-filling rate. Seed disturbance improves seed mobility, thereby enhancing the precision of bunch planting.

Keywords: rice; seed meter; shaped hole; seed disturbance structure; regression model; discrete element



Citation: Qian, C.; He, S.; Qin, W.; Jiang, Y.; Huang, Z.; Zhang, M.; Zhang, M.; Yang, W.; Zang, Y. Influence of Shaped Hole and Seed Disturbance on the Precision of Bunch Planting with the Double-Hole Rice Vacuum Seed Meter. *Agronomy* **2024**, *14*, 768. <https://doi.org/10.3390/agronomy14040768>

Academic Editor: Gniewko Niedbała

Received: 9 March 2024

Revised: 5 April 2024

Accepted: 6 April 2024

Published: 8 April 2024



Copyright: © 2024 by the authors. Licensee MDPI, Basel, Switzerland. This article is an open access article distributed under the terms and conditions of the Creative Commons Attribution (CC BY) license (<https://creativecommons.org/licenses/by/4.0/>).

1. Introduction

Rice is one of the most important food crops in the world, and the main methods used to grow rice are transplanting and direct seeding [1,2]. Direct seeding of rice eliminates the

need for seedling cultivation and transplanting, reduces production costs, and improves production efficiency [3,4]. Mechanized direct seeding of rice can avoid the problems of disordered growth, uneven growth, and lodging associated with manual sowing [5]. Using mechanical seed meters can meet the agronomic requirements of direct seeding of rice bunch planting, but there are problems with large seeding volumes and high seed crush rates [6,7]. The vacuum seed meter has the advantages of high precision of bunch planting, low seed damage rate, and seed saving [8–10]. Using vacuum seed meters in the direct seeding of rice can solve the problems of mechanical meters. However, the rice vacuum seed meter's low and variable seed-fill rates are problematic.

Some researchers have designed vacuum seed meters with different structures and optimized the key components to meet the precision seeding of different crops. The precision plug seeder for vegetables was developed to sow chili and tomatoes [11]. The vacuum seed meter was improved and optimized for mechanized sowing of sandalwood seeds in the diameter range of 13.5 to 23.5 mm [12]. A vacuum seed meter for potatoes was constructed, and the key components were designed and theoretically analyzed [13]. A multi-row pneumatic plate metering device was invented to cope with the sowing of oilseed rape in multiple rows [14]. A peanut precision meter for peanut sowing under mulch conditions was developed [15]. A metering device was developed using internal air pressure to improve the seed-filling rate in the high-speed sowing of maize [16]. A high-speed seed metering device with centrifugal fill and clean was designed for maize at 10 to 20 km/h [17]. For high-density planting of maize, cotton, and sunflower, an intermittent seed meter with a left seed disc and a right seed disc was invented [18]. To increase the working speed in the precision planting of maize, the method of positive pressure air flow and inclined seed disc is used to improve the seed falling speed of the seed meter, and the research proved that the high-speed positive pressure air flow can improve the uniformity of the seed spacing [19]. Seed and meter structure are the main factors affecting sowing accuracy, and some scientists have carried out related research. A mathematical model of the physical characteristics of different seeds (thousand kernel weight, projected area, sphericity, and seed density) with their optimum operating pressure was developed, and validation tests showed that the model could predict the optimum vacuum pressure of the seed meter [20]. The influence of the forward speed, the vacuum pressure, and the entry cone angle of the hole on the seeding accuracy was investigated to optimize the cotton seed meter, and the structure and working parameters were determined [21]. A study was carried out on the effect of different numbers of seed suction holes on seed spacing uniformity based on a computerized measurement system [22]. A prediction model based on artificial neural network multi-objective particle swarm optimization was established to maximize the quality feed index, and the error between the measured and predicted values was 2.11%, proving the model's accuracy [23]. In recent years, it has become common to use numerical simulations to analyze the process of vacuum seeders. Based on computational fluid dynamics (CFD), the gas flow inside the rapeseed seed meter was simulated to determine the factors affecting seeding accuracy [24]. The working process of the inside-filling, air-blowing, seed-metering device was simulated based on CFD and the discrete element method (DEM) to optimize the structure of the seed-metering device [25]. The movement of maize seed in the airflow-assisted seed-dropping device was simulated by CFD and DEM to investigate the influence of the structural parameters of the seed drop tube on the seeding accuracy [26]. A numerical simulation based on CFD-DEM of a vegetable seed meter was carried out to analyze the changes in the flow field and seed movement law, and bench tests were carried out to determine the optimum operating parameters of the seed meter [27].

Currently, research into vacuum seed meters focuses mainly on high sphericity and large seeds such as peanuts, cotton, and maize. However, rice seeds have a fusiform shape and are seeds of low sphericity, having lemma hairs on their surface, resulting in poor seed mobility. The agronomic requirements of rice field direct seeding differ from those of other single-seed crops. Rice field direct seeding is generally used to plant multiple seeds per

hole to ensure the field emergence rate, so that the vacuum seed meter for each group hole has a double-hole structure. Therefore, further research is needed to investigate the effect of structural parameters of vacuum seed meters on the precision of rice bunch planting.

In this paper, the effect of the shaped hole of the meter disc on the precision of rice bunch planting was first investigated, and the optimum shaped hole structure was determined. Then, based on the optimal hole structure, the qualities of feed index, miss index, and multiple index with different seed disturbance structures were analyzed at different vacuum pressures and speeds. Multiple regression models were developed for vacuum pressure, speed, and seed disturbance structure concerning the quality of feed index, miss index, and multiple index.

2. Materials and Methods

2.1. Seed Meter and Test Stand

The vacuum seed meter for rice mainly consists of seed inlet, seed-filling chamber, disc, seal rubber, and vacuum chamber (See Figure 1). The rice vacuum seed meter has 12 groups of seeding holes, each group having double 1.5-mm diameter holes. The seeds enter the seed chamber from the seed inlet, are suctioned by holes under the pressure difference, and then rotate to the release area with the disc to complete the seeding. The test bench, as shown in Figure 2, can adjust and measure the rotational speed of the seed meter through the motor governor and Hall sensor, respectively, and the rotational speed adjustment error is ± 1 rpm. The vacuum pressure of the seed meter can be adjusted and measured through the adjustable fan and the air pressure sensor, respectively, and the vacuum pressure adjustment error is ± 0.05 kPa. The type of Hall sensor and air pressure sensor are the CYT9100HT of TYHC and the QBM3020 of SIEMENS. Different shaped hole structures (see Figure 3) and seed disturbance structures (see Figure 4) were designed to improve the seed-filling rate of the vacuum seed meter.

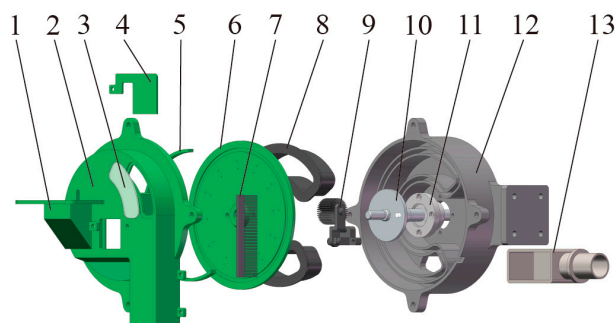


Figure 1. Structural schematics of vacuum seed meter for rice. 1. Seed inlet, 2. Seed chamber, 3. View port, 4. Seed feed adjustment plate, 5. Isolation ring, 6. Disc, 7. Seed pool baffle brush, 8. Seal rubber, 9. Clean brush roller, 10. Axle, 11. Bearing, 12. Vacuum chamber, 13. Air outlet.

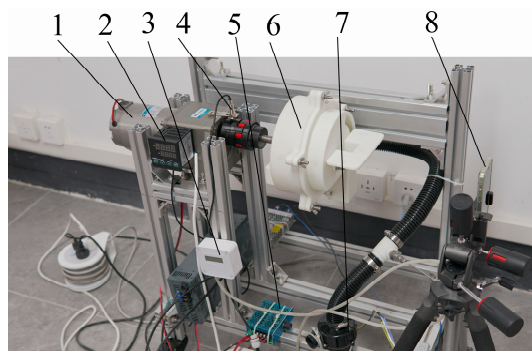


Figure 2. Test bench. 1. Motor, 2. Rotation speed display, 3. Air pressure sensor, 4. Hall sensor, 5. Motor governor, 6. Seed meter, 7. Adjustable fan, 8. Camera.

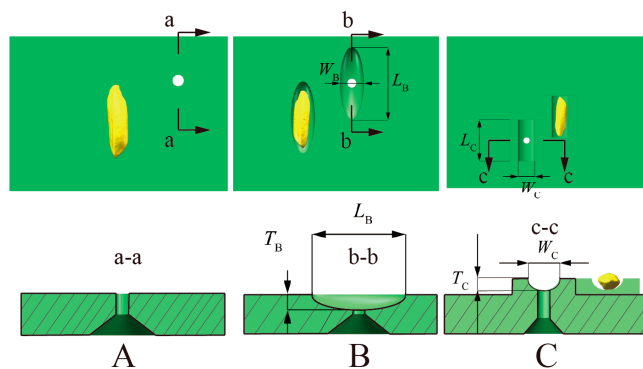


Figure 3. Structural schematic diagram and parameters of holes (A–C).

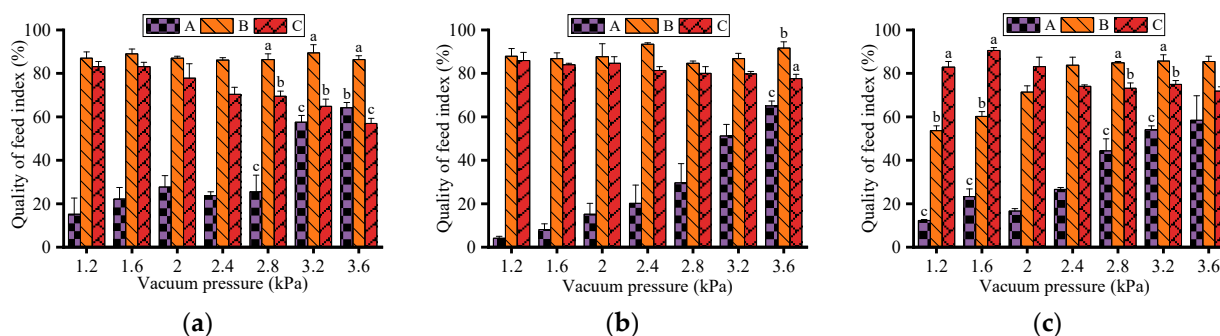


Figure 4. Variation of the quality of feed index for different shaped holes. A, B, and C refer to hole A, hole B, and hole C respectively. Lowercase letters (a, b, and c) indicate significant differences ($p < 0.05$). The same is below. (a) 20 rpm; (b) 40 rpm; (c) 60 rpm.

2.2. Rice Seed

The “Wuyou 1179” indica rice seed with an average water content of <13% was selected as the test material. Rice seeds were between 6.40 mm and 9.72 mm long, 1.83 mm and 2.98 mm wide, and 1.34 mm and 2.31 mm thick. Thousand-grain weight of “Wuyou 1179” was 23.6 g.

2.3. Measurement of Precision of Bunch Planting

The qualities of feed index, miss index, and multiple index were used as indicators to evaluate the precision of rice bunch planting. During the test, the number of seed grains suctioned by each group of holes was recorded; 360 groups of holes were counted in each test, and each test was repeated three times. For each trial, the probability P_i that the seed meter adsorbs a different number of seeds can be calculated according to Equation (1). The quality of feed means that the number of seeds suctioned per group of holes is 1–2. Miss means that the number of seeds suctioned per group of holes is 0. Multiple means that the number of seeds suctioned per group of holes is greater than 2. Hence, the qualities of feed index, miss index, and multiple index are equal to P_{1-2} , P_0 , and $P_{>2}$, respectively:

$$P_i = \frac{\sum X_i}{360}, i = 0, 1, 2, 3, 4 \dots \quad (1)$$

where, P_i is the probability that the seed meter suctioned a number of seeds, and X_i is the number of different seeds suctioned by each set of holes.

2.4. Statistics and Analysis of Data

Data were compiled using Excel 2019 software. One-way ANOVA significance analysis (with $p < 0.05$ defined as a significant difference) and linear regression analysis were performed using SPSS 27 software for experimental data satisfying independence, normal-

ity, and homogeneity of variance. Graphs were generated using Origin 2019b software and discrete element simulation using EDEM 2022.2 software. Data that are not labeled with a lowercase letter are those that do not satisfy normality or homogeneity of variance. Although some of the data appeared to be significantly different, they did not meet the conditions for one-way ANOVA.

3. Effect of the Shaped Hole on the Precision of Bunch Planting

3.1. Shaped Hole

To reduce seed action on suctioned seeds, two types of shaped hole structures were designed as shown in Figure 3. The structural parameters L_B , W_B , and T_B of the shaped hole B are 12 mm, 4 mm, and 2 mm, respectively, and the structural parameters L_C , W_C , and T_C of the shaped hole C are 12 mm, 4 mm, and 1.5 mm, respectively. The hole spacing for direct seeding of rice is generally adjustable from 0.1 to 0.2 m. For the rice precision direct seeding machine using the rice transplanter as the power source, the transplanter field working speed is generally 0–1.3 m/s. There are 12 groups of double-suction holes in the seed meter, and the speed is taken as 20–60 rpm to meet the agronomic requirements of direct seeding of rice. For the test, speeds of 20 rpm, 40 rpm, and 60 rpm were used and the vacuum pressure was 1.2–3.6 kPa, with the vacuum pressure level adjusted by 0.4 kPa.

3.2. Results and Analyses

The variation in the quality of feed index for different holes is shown in Figure 4. At a rotational speed of 20 rpm, the differences in the quality of feed index (QFI) of hole A, hole B, and hole C at vacuum pressures of 2.8 kPa, 3.2 kPa, and 3.6 kPa were significant ($p < 0.05$). At a speed of 40 rpm, there was a significant difference ($p < 0.05$) between the QFI of holes A, B, and C at a vacuum of 3.6 kPa. At a speed of 60 rpm, there was a significant difference ($p < 0.05$) between the QFI of hole A, shaped hole B, and shaped hole C at vacuum pressures of 1.2 kPa, 1.6 kPa, 2.8 kPa, and 3.2 kPa. When the rotation speed is 20 rpm, 40 rpm, and 60 rpm, the QFI of hole A tends to increase with increasing vacuum. At 1.2 kPa to 2.8 kPa, the QFI of hole A is less than 50%. The QFI of hole A is lower because hole A has no shaped hole structure, it is difficult to break the seed stacking state, and the suctioned seeds are easily released from the hole under the friction between the seeds. A higher vacuum is required to increase the seed-filling rate of hole A. When the speed is 20 rpm and 40 rpm, the QFI of shaped hole B does not show a significant change trend with the increased vacuum. At a speed of 60 rpm, as the vacuum increases, the QFI of shaped hole B tends to increase and stabilize first. The main reason for this trend in QFI of shaped hole B is that the shaped hole B hole is an elliptically grooved hole that maintains a stable seed posture during the filling process, thus reducing the influence of seeds on the suctioned seed. The quality of feed index of shaped hole C showed an overall decreasing trend with increasing vacuum at 20 rpm, 40 rpm, and 60 rpm. The shaped hole C with the elliptical convex stand has a specific disturbing effect on the seeds, which can facilitate seed suction. However, the phenomenon of non-suctioned seeds being carried by the front end of the elliptical convex stand may occur, so that the phenomenon of the multiple index increases as the vacuum increases.

The multiple index of hole B and hole C tended to increase with increasing vacuum at speeds of 20 rpm, 40 rpm, and 60 rpm (see Figure 5). This trend is mainly due to an increase in vacuum pressure, which leads to an increase in suction force and, therefore, an increase in multiple index. Among them, the multiple index of shaped hole C is higher than the other two, and the increase in the multiple index of shaped hole B is smaller than that of shaped hole C. The multiple index of hole A fluctuates wildly. The shaped hole C hole structure is higher than the disc surface. Rice seeds that are not suctioned when rotating with the disc will be carried by the shaped hole to the seed releasing area, resulting in too high a multiple index for the shaped hole C. Seeds that are suctioned in hole A at low speeds may be dislodged from the hole by the extrusion of the population, so the multiple index of hole A is low. However, the same hole suctioned a few seeds to form a stable seed mass at

high speeds, and population extrusion had less effect on it, so the multiple index of hole A was more significant at high speeds. The reason for the more stable multiple index of the shaped hole B is that the structure of the holes gives the seeds a stable posture when filled with seed. At a speed of 20 rpm, there were significant differences ($p < 0.05$) in the multiple index of hole A, shaped hole B, and shaped hole C at vacuum pressures of 2.4 kPa and 2.8 kPa; and between hole A and shaped hole C at vacuum pressure of 1.6 kPa. At a speed of 40 rpm, there was a significant difference ($p < 0.05$) in the multiple index of hole A, hole B, and hole C at a vacuum of 1.6 kPa, and hole B differed significantly ($p < 0.05$) from hole A and hole C at a vacuum of 3.6 kPa. At a speed of 60 rpm, the difference in the multiple index between hole C and hole A, and between hole C and hole B at vacuum pressures of 2 kPa and 2.8 kPa was significant ($p < 0.05$), and the difference between the multiple index of hole A, hole B, and hole C and at vacuum pressure of 3.2 kPa was significant ($p < 0.05$).

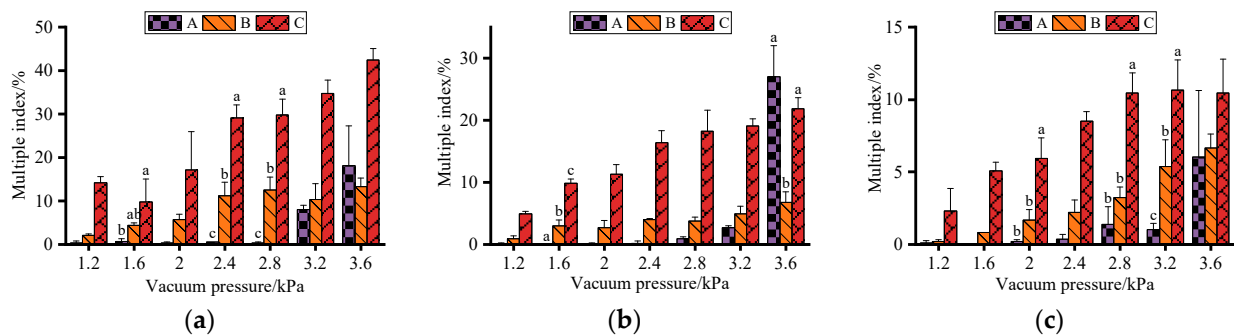


Figure 5. Variation of multiple index for different shaped holes: (a) 20 rpm; (b) 40 rpm; (c) 60 rpm. A, B, and C refer to hole A, hole B, and hole C respectively. Lowercase letters (a, b, and c) indicate significant differences ($p < 0.05$).

As shown in Figure 6, the miss index tends to decrease with the increase of vacuum, and the miss index of hole A is higher than that of shaped hole B and shaped hole C. The miss index of shaped hole C is the lowest. The main reason for this trend is that hole A has no shaped hole structure, and the seeds have no stable posture to be influenced by the population during the filling process, which leads to its high miss index. When the rotational speed is 20 rpm and the vacuum is 2.4 kPa to 3.6 kPa, the miss index of shaped hole B is less than 3%, and the miss index of shaped hole C is less than 1%. The differences in the miss index of hole A, hole B, and hole C at a vacuum of 1.6 kPa at a speed of 60 rpm were significant ($p < 0.05$).

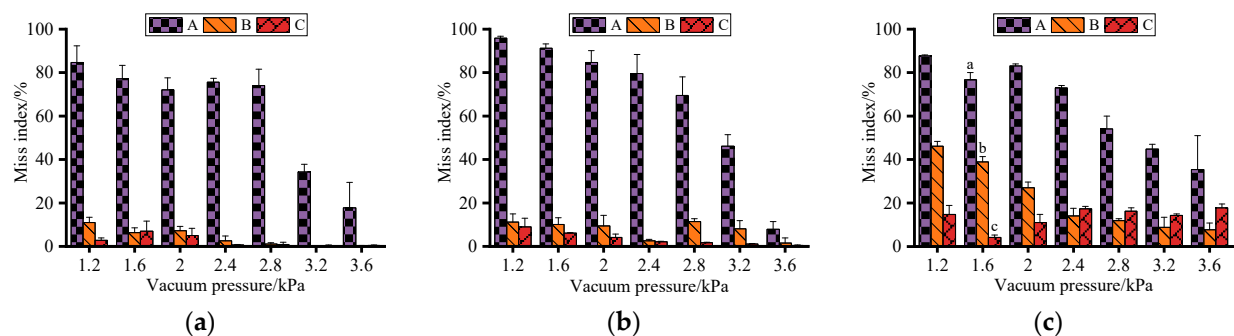


Figure 6. Variation of miss index for different shaped holes: (a) 20 rpm; (b) 40 rpm; (c) 60 rpm. A, B, and C refer to hole A, hole B, and hole C respectively. Lowercase letters (a, b, and c) indicate significant differences ($p < 0.05$).

Figure 7 shows that the suctioned seeds on shaped hole A have no stable posture and the contact area between the seeds and the hole is small. The suctioned seeds on hole B have a more stable posture, and hole C shows the phenomenon of some of the seeds

stacking. The shaped hole structure allows the seeds to maintain a stable posture during the seed-filling process and reduces the influence of the population on the suctioned seeds. The stabilized seed suction posture is conducive to improving the precision of bunch planting. According to the above analysis, shaped hole structures have an effect on the quality of feed index, miss index, and multiple index. Compared with the other two shaped hole structures, the QFI of hole B is higher than that of hole A and hole C, and the QFI of hole B is stable; the multiple index of hole B is lower than that of hole C, and the miss index of hole B is lower than hole A. Seeds on hole A are easily detached from the suction hole by the action of other seeds. The shaped hole structure of hole B reduces the action of other seeds on the seeds of hole B. Additional edges of the shaped hole C carry excess seed. Therefore, the shaped hole B was selected as the shaped hole for the rice vacuum seed meter in the following tests.

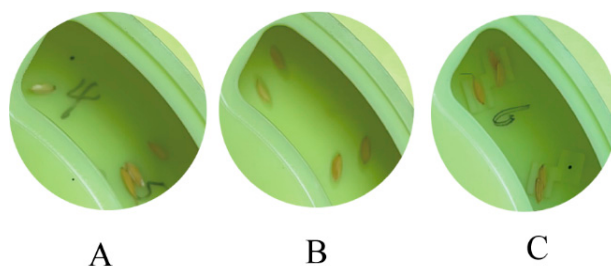


Figure 7. Seed suction posture of different holes at a speed of 40 rpm and vacuum of 2.8 kPa. A, B, and C refer to hole A, hole B, and hole C respectively.

4. Effect of the Seed Disturbance Structure on the Precision of Bunch Planting

4.1. Seed Disturbance Structure

Based on the optimal shaped hole structure, seed disturbance structures (SDS) were designed as shown in Figure 8. SDS IV, SDS V, and SDS VI are composed of SDS I, SDS II, and SDS III, plus a seed guidance strip, respectively. The main structural parameters R_1 , R_2 , θ_1 , θ_2 , and H_1 of SDS I and SDS IV are 40 mm, 58 mm, 25° , 25° , and 1 mm, respectively. The main structural parameters R_3 , R_4 , θ_3 , θ_4 , and H_2 of SDS II and SDS V are 78 mm, 58 mm, 20° , 12° , and 1 mm respectively. The main structural parameters L_1 , L_2 , and L_3 of SDS III, and SDS VI are 25 mm, 6 mm, and 6 mm, respectively. The main structural parameters of the seed guidance strip were 6 mm, 1 mm, and 1.5 mm for L_4 , W , and H_4 , respectively. The rotational speed was taken as 20–60 rpm and the vacuum pressure as 1.2–3.6 kPa.

4.2. Results and Analyses

When the speed was 20 rpm, the QFI of discs with different seed disturbance structures showed different trends with increasing vacuum (see Figure 9a). Among them, the QFI of SDS III, SDS IV, SDS V, and SDS VI showed a decreasing trend with the increase of vacuum pressure. On the one hand, this was because the longer filling time at low speeds is favorable for seed filling, and on the other hand, it was because the optimum QFI of SDS III, SDS IV, SDS V, and SDS VI had a vacuum pressure of less than 1.2 kPa. The QFI of SDS I and SDS II showed a dynamic change, first increasing and then decreasing with the increase of vacuum. This was because the increase of vacuum improved the suction force of the holes to improve the seed-filling performance of the seed meter and when the vacuum reached the optimal QFI of vacuum, the multiple index increased with the increase of vacuum. At a vacuum pressure of 2.0 kPa, the QFI of SDS I was 90.74%, significantly higher than that of SDS II, SDS III, SDS V, and SDS VI ($p < 0.05$). At a vacuum pressure of 2.4 kPa, the QFI of SDS I was 90.56%, significantly higher than that of SDS III, SDS IV, SDS V, and SDS VI ($p < 0.05$).

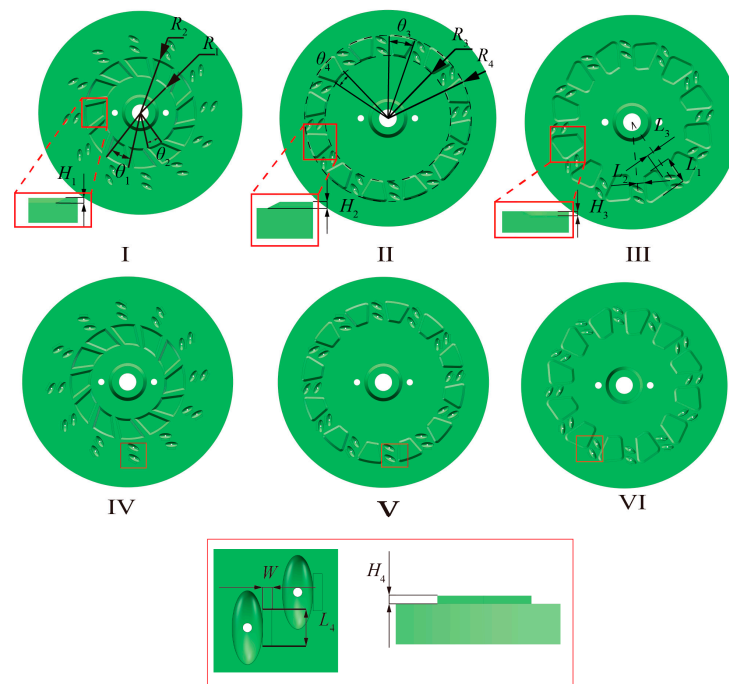


Figure 8. Structural schematic diagram and key parameters of seed disturbance structure. I, II, III, IV, V, and VI refer to SDS I, SDS II, SDS III, SDS IV, SDS V, and SDS VI, respectively.

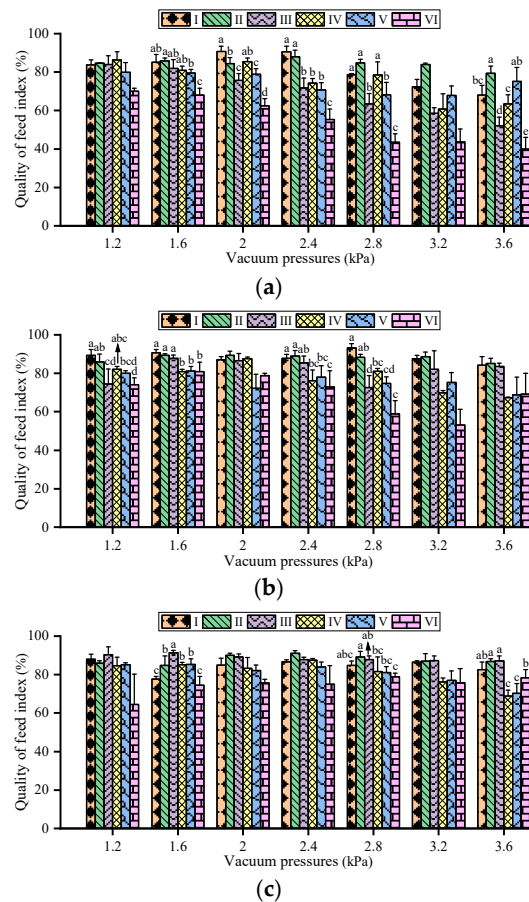


Figure 9. Variation of the quality of feed index for different seed disturbance structures: (a) 20 rpm; (b) 40 rpm; (c) 60 rpm. I, II, III, IV, V, and VI refer to SDS I, SDS II, SDS III, SDS IV, SDS V, and SDS VI, respectively. Lowercase letters (a, b, and c) indicate significant differences ($p < 0.05$).

At a speed of 40 rpm, SDS I and SDS II had higher QFI than the other seed disturbance structures and higher than those at 20 rpm (see Figure 9b). This is mainly due to the increase in rotational speed, which increases the disturbance of the seed population by SDS I and SDS II, improving the flowability of the seeds and allowing the shaped holes to suction the seeds more easily. At a vacuum pressure of 2.4 kPa, the QFI of SDS II was 89.07%, significantly higher than that of SDS IV, SDS V, and SDS VI ($p < 0.05$). At a vacuum pressure of 2.8 kPa, the QFI of SDS I was 93.15%, significantly higher than that of SDS III, SDS IV, SDS V, and SDS VI ($p < 0.05$).

With the change of vacuum, the QFI of various SDS at the speed of 60 rpm shows a more stable trend, even higher than the QFI at low speed (see Figure 9c). This change is partly due to the reduced multiple index of the seed meter at high speeds and partly due to the excellent seed-filling performance of the seed meter with SDS, even at high speeds. The QFI of SDS IV, SDS V, and SDS VI were lower than the other SDS because they had seed guidance strips that made excess seeds enter the holes. Of these, the QFI of SDS II were 90%, 91.11%, and 89.17% at vacuum pressures of 2.0 kPa, 2.4 kPa, and 2.8 kPa, respectively. At vacuum pressures of 1.2 kPa, 1.6 kPa, and 2.0 kPa, the QFI of SDS III were 90.37%, 91.30%, and 89.17%, respectively. At a vacuum pressure of 1.6 kPa, the QFI of SDS III was significantly higher than that of SDS I, SDS II, SDS IV, SDS V, and SDS VI ($p < 0.05$). At a vacuum pressure of 2.8 kPa, the QFI of SDS III was significantly higher than that of SDS IV, SDS V, and SDS VI ($p < 0.05$).

When the speed of the seed meter was 20 rpm, the multiple index of the seed disks with different SDS tended to increase approximately with the increase in vacuum (see Figure 10a). Among them, the multiple index of SDS VI was higher than the other SDS, ranging from 28.98% to 59.81%, indicating that the seed-filling performance of SDS VI was due to the other SDS. This is mainly because the groove structure of the SDS VI and the seed guidance strip can make more seeds flow near the holes to increase the seed-filling rate. When the vacuum was 1.2 kPa to 2.4 kPa, the multiple index of the SDS I was the lowest; when the vacuum was 2.8 kPa to 3.6 kPa, the multiple index of the SDS II was the lowest.

With the change of vacuum pressure, the multiple index of SDS II at 40 rpm showed an increasing trend with the increase of vacuum pressure, while the multiple index of the other SDS showed a fluctuating trend with the increase of vacuum pressure (see Figure 10b). Among them, the multiple index of SDS II was lower than other SDS at vacuum pressures of 1.6 kPa, 2.0 kPa, 2.4 kPa, 3.2 kPa, and 3.6 kPa. At a vacuum pressure of 2.8 kPa, the multiple index of SDS VI was significantly higher than that of SDS I, SDS II, SDS III, SDS IV, and SDS V ($p < 0.05$).

When the rotational speed was 60 rpm, the multiple index of various SDS showed a fluctuating trend with the change in vacuum (see Figure 10c). Among them, the multiple index of SDS II showed an increasing trend with the increase of vacuum pressure, and the multiple index of SDS II ranged from 2.96% to 12.31%, while the multiple index of SDS II was smaller than that of other structures at vacuum pressures of 1.6 kPa, 2.0 kPa, 2.4 kPa, 3.2 kPa, and 3.6 kPa. The multiple indexes of SDS IV, SDS V, and SDS VI were higher than the rest of the multiple indexes, probably because these three structures have a guidance strip that makes it easier for the seed to flow to the shaped hole at high rotational speeds.

At the same speed, the miss index of the seed meter disc with different SDS showed a decreasing trend with increasing vacuum (see Figure 11). At a rotational speed of 20 rpm, the miss index (<1%) of the SDS VI was smaller than that of the other SDS, mainly because the SDS VI was more accessible for seeds to be suctioned by the hole compared to the other structures. When the vacuum pressure was 2 kPa to 3.6 kPa, the miss index of the seed meter disk with disturbance seed structure was less than 6%. When the vacuum pressure was 2.4 kPa to 3.6 kPa, the miss index of SDS II, SDS III, SDS IV, and SDS V was less than 2.5%. When the rotational speed was 40 rpm and the vacuum pressure range 2.0 kPa to 3.6 kPa, the miss indexes of SDS I, SDS II, SDS III, SDS IV, SDS V, and SDS VI were less than 4%. Vacuum pressures of 1.2 kPa and 1.6 kPa resulted in significantly higher miss index

than vacuum pressures of 2.0 kPa to 3.6 kPa, primarily because the vacuum pressure to maintain stable seed filling of the seed meter at a speed of 40 rpm should be greater than 1.6 kPa. When the rotational speed was 60 rpm and the vacuum pressure ranges 2.4 kPa to 3.6 kPa, the miss indexes of SDS II, SDS III, SDS IV, SDS V, and SDS VI were less than 5%. The miss index of the SDS II was less than 3% in the vacuum range of 2.0 kPa to 3.6 kPa. At a vacuum pressure of 1.6 kPa, the miss index of SDS I was significantly higher than that of SDS II, SDS III, SDS, SDS V, and SDS VI ($p < 0.05$).

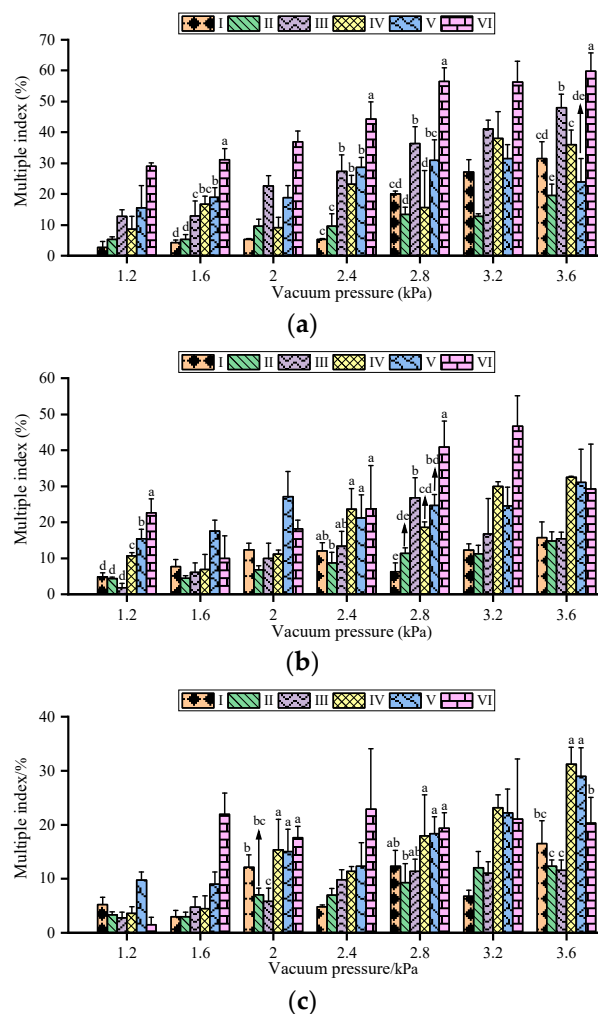


Figure 10. Variation of multiple index for different seed disturbance structures: (a) 20 rpm; (b) 40 rpm; (c) 60 rpm. I, II, III, IV, V, and VI refer to SDS I, SDS II, SDS III, SDS IV, SDS V, and SDS VI, respectively. Lowercase letters (a, b, and c) indicate significant differences ($p < 0.05$).

At speeds of 20 rpm and 40 rpm, seed disturbance structure I and seed disturbance structure II had higher quality of feed index. At speeds of 60 rpm, seed disturbance structure II and seed disturbance structure III had a higher quality of feed index. The multiple indexes of seed disturbance structures I and II were lower than the rest. However, at a speed of 60 rpm, the seed disturbance structure I had a high miss index. In conclusion, the precision of rice bunch planting of the seed disturbance structure II is optimal. Figures 4c and 9c show that the quality of feed index of the seed disc with seed disturbance structure is significantly higher than that of the seed disc without seed disturbance structure at high speed, and the quality of the feed index changes are stable. Meanwhile, at the same speed and under vacuum pressure, the multiple index of the seed disc with the seed disturbance structure was higher than that of the seed disc without the seed disturbance structure, and the miss index of each of the seed disturbance structures was lower than that without the

seed disturbance structure. In summary, the seed-filling performance of the seed meter with the seed disturbance structure is in all ways better than that of the seed meter without the seed disturbance structure. At a speed of 60 rpm and a vacuum pressure of 2.4 kPa, the seed suction posture of each seed disturbance structure is shown in Figure 12. It can be seen from Figure 12 that seeds suctioned by the meter disc with seed disturbance structure are maintained in a stable suction posture.

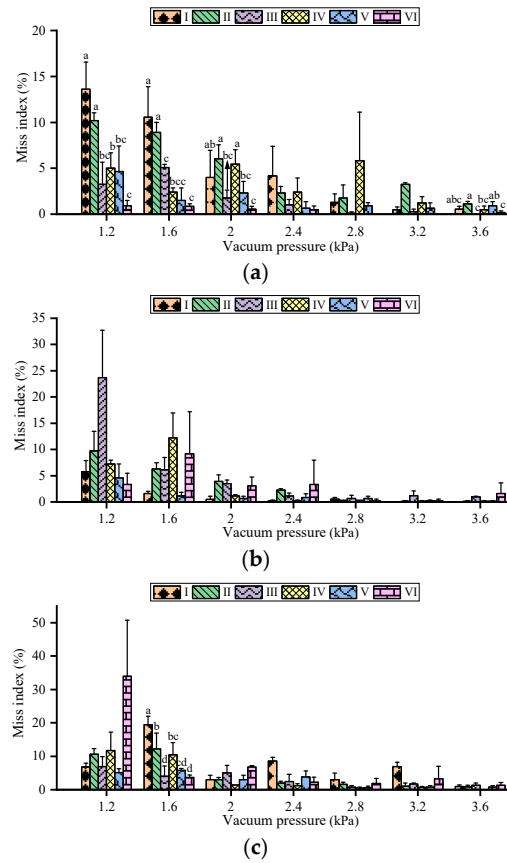


Figure 11. Variation of miss index for different seed disturbance structures: (a) 20 rpm; (b) 40 rpm; (c) 60 rpm. I, II, III, IV, V, and VI refer to SDS I, SDS II, SDS III, SDS IV, SDS V, and SDS VI, respectively. Lowercase letters (a, b, and c) indicate significant differences ($p < 0.05$).

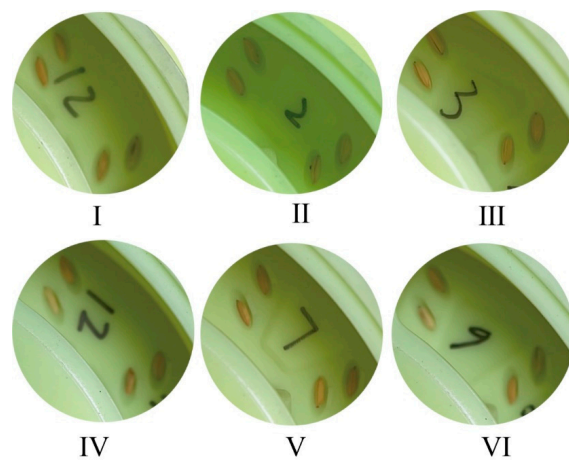


Figure 12. Seed suction posture of different disturbance structures at a speed of 60 rpm and vacuum pressure of 2.4 kPa. I, II, III, IV, V, and VI refer to SDS I, SDS II, SDS III, SDS IV, SDS V, and SDS VI, respectively.

4.3. Multiple Regression Models

Multiple linear regression analyses were carried out with the experimental results of the effect of seed disturbance structure on the precision of bunch planting to investigate the relationship between speed, vacuum, and seed disturbance structure and precision of bunch planting. Since seed disturbance structure is a categorical variable, the multiple linear regression analyses were performed with the seed disturbance structure set as five dummy variables and the seed disturbance structure VI as the reference group. The multiple regression equations for the quality of feed index, miss index, and multiple index are shown in Equation (2):

$$Y_i = \beta_0 + \beta_1 X_1 + \beta_2 X_2 + \beta_3 D_1 + \beta_4 D_2 + \beta_5 D_3 + \beta_6 D_4 + \beta_7 D_5 + \mu_i \quad (2)$$

where, Y_i denotes the quality of feed index, miss index, and multiple index of the seed meter; β_1 to β_7 denote coefficients; μ_i is the random error; X_1 and X_2 are speed and vacuum, respectively; D_1 – D_5 denote the dummy variables for the disturbance structure I–V. D_1 to D_5 are taken as 0 or 1, if one of the dummy variables is 1, the rest of the dummy variables are 0. If D_1 – D_5 are all 0, the model is a disturbance structure VI.

Regression analyses were performed, and the multiple regression model was obtained, as shown in Table 1. The ANOVA results of the regression model are presented in Table 2. The regression models must be diagnosed to ensure their accuracy. The residuals of the regression model must follow a normal distribution, and the independent variables of the model should be free of multicollinearity. The VIF value of the independent variable is less than 5, which means there is no multicollinearity between the variables, and it does not affect the accuracy of the regression results. Figure 13 shows that the residuals of the QFI model and the multiple model obey a normal distribution, so they are accurate. However, the miss index model does not follow a normal distribution (see Figure 13c). Therefore, the miss index regression model is not statistically significant. The ANOVA results showed that the p values of the QFI model and the multiple model were all less than 0.01, indicating that the regression models are significant. The R^2 of the regression models for the quality of feed index and multiple index were 0.65 and 0.73, indicating that the fit of the regression models for the quality of feed index and multiple index was 65% and 73%.

Table 1. Regression models of quality of feed index and multiple index.

Model	VIF	Coefficient		SD		Significance	
	All	QFI	Multiple	QFI	Multiple	QFI	Multiple
Constant		67.51	22.48	2.63	2.67		
Speed	1.00	0.24	−0.29	0.04	0.04		
Vacuum	1.00	−4.45	7.93	0.72	0.73		
SDS I	1.67	18.42	−19.13	1.99	2.02	<0.01	<0.01
SDS II	1.67	20.39	−20.89	1.99	2.02		
SDS III	1.67	13.69	−13.40	1.99	2.02		
SDS IV	1.67	11.83	−11.50	1.99	2.02		
SDS V	1.67	10.56	−8.78	1.99	2.02		

Table 2. ANOVA of regression models for quality of feed index and multiple index.

Model		Sum of Squares	df	F	p	R ²
QFI	Regression	8947.4	7	30.74	<0.01	0.65
	Residual	4906.37	118			
Multiple	Regression	13,853.68	7	46.27	<0.01	0.73
	Residual	5046.82	118			

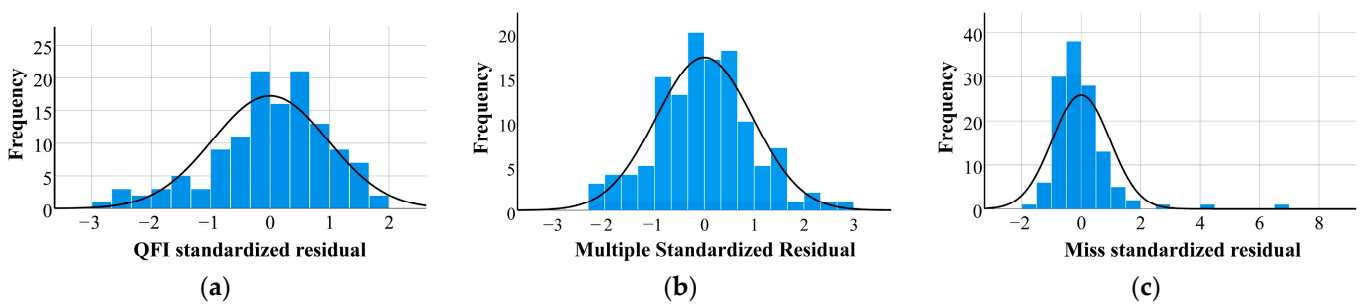


Figure 13. Histogram of standardized residuals for regression models: (a) QFI; (b) multiple; (c) miss.

4.4. Discrete Element Simulation

The discrete element model of rice seed and seed meter is shown in Figure 14. The Poisson ratios of rice seed and seed meter are 0.25 and 0.42, the densities are 1045 kg/m^3 and 1120 kg/m^3 , and the shear moduli are $1.08 \times 10^8 \text{ Pa}$ and $2.70 \times 10^9 \text{ Pa}$, respectively. The restitution coefficient, static friction coefficient, and rolling friction coefficient between seed and seed meter are 0.25, 0.5, and 0.01, respectively. The restitution coefficient, static friction coefficient, and rolling friction coefficient between seed and seed meter are 0.52, 0.48, and 0.01, respectively [28].

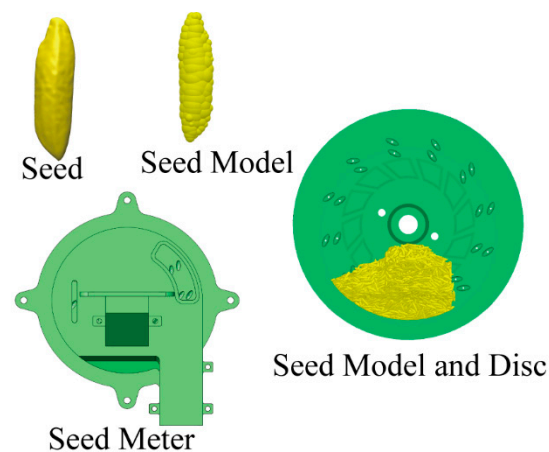


Figure 14. Seed meter model and rice seed model in discrete element simulation.

The velocity and force magnitude of seeds are applied to indicate the amount of disturbance. After the simulation is completed, the velocity magnitude and force magnitude variation data of the seed discrete element model are derived at 0.01 s time interval, and the average velocity magnitude and average force magnitude within 4–10 s of the simulation time are used as evaluation indices of the disturbance.

Discrete element simulations were performed to obtain the total force magnitude of the seed for different meter discs, as shown in Figure 15a. The total force magnitude of the seed was positively correlated with speed in the rows of seed discs, except for CK. The main reason is that the higher the speed, the more the seeds are disturbed by the discs with a disturbance structure. In contrast, without the disturbance structure, the CK cannot break the stacked state of seeds despite the increase in speed. At 40 rpm and 60 rpm, the total force magnitude on the seeds with the disturbance structure of the seed discs was significantly higher than the CK. The velocity magnitude of the seed during the operation of the different meter discs is shown in Figure 15b. The velocity magnitude of the meter discs with disturbance structure increases with increasing speed, but the velocity magnitude of the CK at 60 rpm is lower than the velocity magnitude at 20 rpm. The main reason for this phenomenon is the disturbance structure of the disc that disturbs the seed pile. Disturbance increases with the speed of rotation. However, due to the CK disc without

the disturbance structure, the seeds appear to have a stacked state earlier at high speeds than at low speeds. Figure 16 shows the seed velocity vector of different meter discs at a simulation time of 5 s. It can be seen that the seeds of the CK disc are in a stacked state, and the poor seed mobility of the CK disc is not conducive to seed filling. The seed mobility of the meter disc with the disturbance structure is better, and the seed speed around the hole is significantly higher than that of the control group.

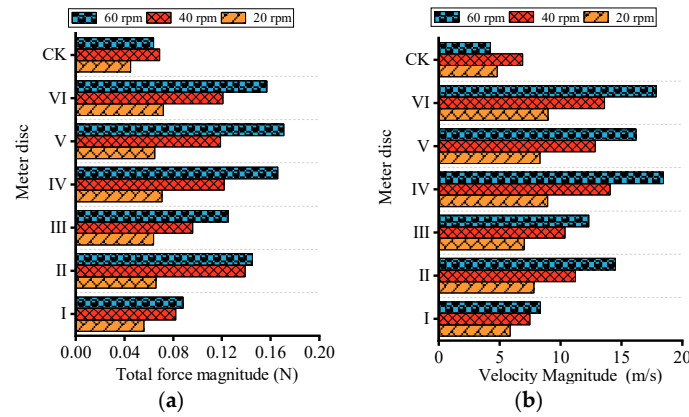


Figure 15. Total force and velocity magnitude for different meter discs: (a) total force; (b) velocity magnitude. I, II, III, IV, V, VI, and CK refer to SDS I, SDS II, SDS III, SDS IV, SDS V, SDS VI, and without SDS, respectively.

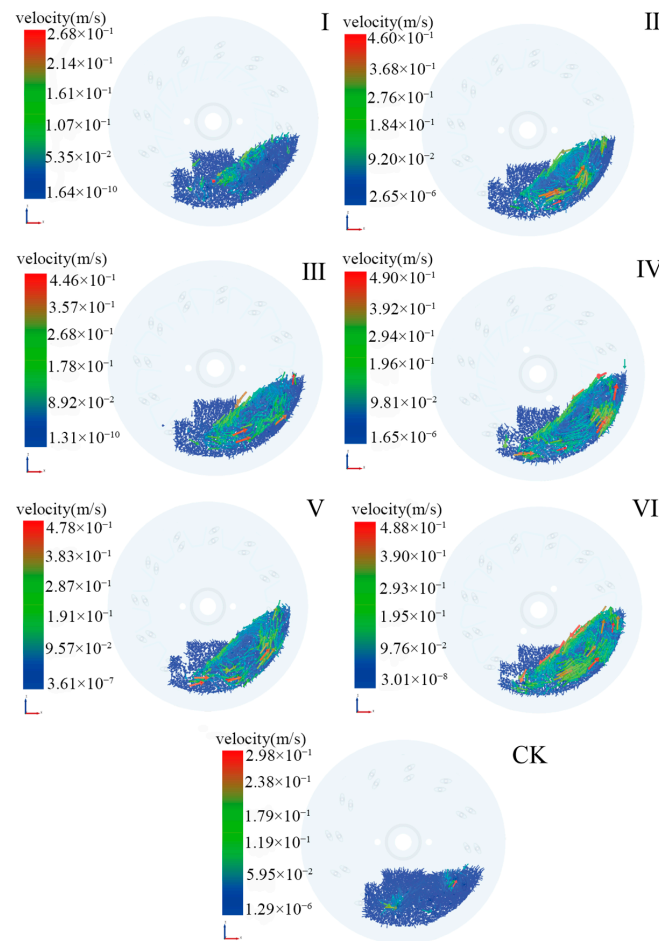


Figure 16. Seed velocity vector of different meter discs at 60 rpm. I, II, III, IV, V, VI, and CK refer to SDS I, SDS II, SDS III, SDS IV, SDS V, SDS VI, and without SDS, respectively.

5. Discussion

This study shows a difference in the precision of rice bunch planting between seed meters with different shaped hole structures. The seed meter with shaped holes had a higher quality of feed index than the seed meter without shaped holes, and the miss index was much lower than that of the seed meter without shaped holes. Some studies have found that the shaped hole structure can improve the planting precision of mechanical seed meters, which is consistent with the results of this paper [29,30]. A seed meter with a shaped hole structure allows the seeds to maintain a stable suction posture during the filling process, preventing the suctioned seeds from being dislodged from the holes by the action of the seeds. A stable seed suction posture is conducive to improving the seed filling rate of the seed meter. For seeds with low sphericity, the shaped hole structure of the meter disc can be used to improve the precision of bunch planting of the seed vacuum meter [31].

The quality of the feed index of the seed meter with the disturbance structure has low fluctuation. At high speed, the quality of the feed index of the seed meter with the disturbance structure is significantly higher than that of the seed meter without the disturbance structure. The miss index of the seed meter with the disturbance structure is lower than that of the seed meter without the disturbance structure, and there is a lower miss index even at high speeds. The seed disturbance structure improves the seed-filling performance of the oilseed rape seed meter as reported in [32]. Rice seeds are less mobile than oilseed rape seeds. Differences in the quality of feed index, miss index, and multiple index of seeders with different disturbance structures are mainly due to differences in the mobility of seeds with different disturbance structures. Seed meters with a disturbance structure can break up the seed stacked state and maintain good seed mobility during filling. Seeds in the seed meter without a disturbance structure are prone to pile up. Seed disturbance improves seed mobility and makes seeds more easily suctioned. For seeds with poor mobility, seed meter discs with disturbance structures can improve the precision of bunch planting.

The optimized seed meter performed better regarding the quality of the feed index and the miss index, but the multiple index was high. Further studies need to optimize the seed meter to reduce the multiple index. It is also necessary to consider the effect of machine vibration on the seed meter.

6. Conclusions

This study investigated the effect of shaped holes and seed disturbance structure on the precision of rice bunch planting using a double-hole vacuum seed meter as the research object. First, when the rotational speed is 20–60 rpm, and the vacuum pressure is 1.2–3.6 kPa, the quality of the feed indexes of hole structures, in descending order, are hole B, hole C, and hole A. The miss index of hole A is the highest, and the multiple index of hole C is the highest. Hole B is the optimum structure. Holes B and C have a shaped hole structure. Thus, the precision of rice bunch planting with the shaped hole structure was much higher than that without the shaped hole structure. The shaped hole structure enables a stable suction posture to be maintained during seed filling and improves the seed-filling performance of the seed meter.

There were differences in the planting precision of the different seed disturbance structures, with the highest multiple index in the seed disturbance structure VI, the highest miss index in the seed disturbance structure I, and the optimum structure being the seed disturbance structure II. At a speed of 60 rpm and vacuum pressures of 2.0 kPa, 2.4 kPa, and 2.8 kPa, the quality of feed indexes of seed disturbance structure II were 90%, 91.11%, and 89.17%, respectively, and the miss indexes were 2.96%, 1.94%, and 1.57%, respectively. At high speeds, the planting precision of the seed meter was significantly higher with the seed disturbance than without the seed disturbance. A regression model with statistical significance was developed to describe the relationship between the speed, the vacuum, the disturbance structure, and the precision of rice bunch planting. Discrete element simulation tests showed that the magnitude of force and velocity of the seeds

with the seed disturbance structure was significantly higher than those without the seed disturbance structure. The seed disturbance structure improves seed mobility and increases the precision of bunch planting.

Author Contributions: Conceptualization, Y.Z. and W.Y.; methodology, C.Q.; software, S.H. and Z.H.; validation, W.Q., Y.J. and Z.H.; formal analysis, C.Q.; investigation, C.Q., Y.J. and W.Q.; resources, Y.Z., M.Z. (Minghua Zhang) and W.Y.; data curation, C.Q. and M.Z. (Meilin Zhang); writing—original draft preparation, C.Q.; writing—review and editing, W.Y. and Y.Z.; visualization, M.Z. (Meilin Zhang); supervision, Y.Z., M.Z. (Minghua Zhang) and W.Y.; project administration, W.Y. and M.Z. (Minghua Zhang); funding acquisition, M.Z. (Minghua Zhang) and Y.Z. All authors have read and agreed to the published version of the manuscript.

Funding: This research was funded by the Guangdong Province Key Field Research and Development Program, Grant numbers 2023B0202130001, the National Natural Science Foundation of China, grant numbers 52175228, Guang Dong Basic and Applied Basic Research Foundation, grant numbers 2020A1515110225, China Agriculture Research System for rice CARS-01, and the Laboratory of Lingnan Modern Agriculture Project, grant numbers NT2021009.

Data Availability Statement: Data are reported within the article.

Conflicts of Interest: The authors declare no conflicts of interest.

References

- Zhang, M.; Wang, Z.; Luo, X.; Zang, Y.; Yang, W.; Xing, H.; Wang, B.; Dai, Y. Review of precision rice hill-drop drilling technology and machine for paddy. *Int. J. Agric. Biol. Eng.* **2018**, *11*, 1–11. [\[CrossRef\]](#)
- Tao, Y.; Chen, Q.; Peng, S.; Wang, W.; Nie, L. Lower global warming potential and higher yield of wet direct-seeded rice in Central China. *Agron. Sustain. Dev.* **2016**, *36*, 24. [\[CrossRef\]](#)
- Li, H.; Zhao, C.; Yan, B.; Ling, L.; Meng, Z. Design and Verification of the Variable Capacity Roller-Wheel Precision Rice Direct Seed-Metering Device. *Agronomy* **2022**, *12*, 1798. [\[CrossRef\]](#)
- Li, H.; Zeng, S.; Luo, X.; Fang, L.; Liang, Z.; Yang, W. Design, DEM Simulation, and Field Experiments of a Novel Precision Seeder for Dry Direct-Seeded Rice with Film Mulching. *Agriculture* **2021**, *11*, 378. [\[CrossRef\]](#)
- Liu, H.; Hussain, S.; Zheng, M.; Peng, S.; Huang, J.; Cui, K.; Nie, L. Dry direct-seeded rice as an alternative to transplanted-flooded rice in Central China. *Agron. Sustain. Dev.* **2015**, *35*, 285–294. [\[CrossRef\]](#)
- Guo, J.; Yang, Y.; Memon, M.S.; Tan, C.; Wang, L.; Tang, P. Design and simulation for seeding performance of high-speed inclined corn metering device based on discrete element method (DEM). *Sci. Rep.* **2022**, *12*, 19415.
- Wang, B.; Na, Y.; Liu, J.; Wang, Z. Design and evaluation of vacuum central drum seed metering device. *Appl. Sci.* **2022**, *12*, 2159. [\[CrossRef\]](#)
- Xing, H.; Wang, Z.; Luo, X.; He, S.; Zang, Y. Mechanism modeling and experimental analysis of seed throwing with rice pneumatic seed metering device with adjustable seeding rate. *Comput. Electron. Agric.* **2021**, *188*, 105697. [\[CrossRef\]](#)
- Tang, H.; Guan, T.; Xu, F.; Xu, C.; Wang, J. Test on adsorption posture and seeding performance of the high-speed precision dual-chamber maize metering device based on the seed characteristics. *Comput. Electron. Agric.* **2023**, *216*, 108471. [\[CrossRef\]](#)
- He, S.; Zang, Y.; Huang, Z.; Tao, W.; Xing, H.; Qin, W.; Jiang, Y.; Wang, Z. Design of and Experiment on a Cleaning Mechanism of the Pneumatic Single Seed Metering Device for Coated Hybrid Rice. *Agriculture* **2022**, *12*, 1239. [\[CrossRef\]](#)
- Gaikwad, B.B.; Sirohi, N.P.S. Design of a low-cost pneumatic seeder for nursery plug trays. *Biosyst. Eng.* **2008**, *99*, 322–329. [\[CrossRef\]](#)
- St Jack, D.; Hesterman, D.C.; Guzzomi, A.L. Precision metering of *Santalum spicatum* (Australian Sandalwood) seeds. *Biosyst. Eng.* **2013**, *115*, 171–183. [\[CrossRef\]](#)
- Lü, J.; Yang, Y.; Li, Z.; Sang, Q.; Li, J.; Liu, Z. Design and experiment of an air-suction potato seed metering device. *Int. J. Agric. Biol. Eng.* **2016**, *9*, 33–42.
- Ilbrahim, E.; Liao, Q.; Wang, L.; Liao, Y.; Yao, L. Design and experiment of multi-row pneumatic precision metering device for rapeseed. *Int. J. Agric. Biol. Eng.* **2018**, *11*, 116–123.
- Kang, J.; Peng, Q.; Zhang, C.; Zhang, N.; Fang, H. Design and testing of a punching-on-film precision hole seeder for peanuts. *Trans. ASABE*. **2020**, *63*, 1685–1696. [\[CrossRef\]](#)
- Du, X.; Liu, C. Design and testing of the filling-plate of inner-filling positive pressure high-speed seed-metering device for maize. *Biosyst. Eng.* **2023**, *228*, 1–17. [\[CrossRef\]](#)
- Li, C.; Zhang, D.; Yang, L.; He, X.; Li, Z.; Jing, M.; Dong, J.; Xing, S. Design and experiment of a centrifugal filling and cleaning high-speed precision seed metering device for maize. *J. Cleaner Prod.* **2023**, *426*, 139083. [\[CrossRef\]](#)
- Degirmencioglu, A.; Cakmak, B.; Yazgi, A. Prototype twin vacuum disk metering unit for improved seed spacing uniformity performance at high forward speeds. *Turk. J. Agric. For.* **2018**, *42*, 195–206. [\[CrossRef\]](#)

19. Tang, H.; Xu, F.; Guan, T.; Xu, C.; Wang, J. Design and test of a pneumatic type of high-speed maize precision seed metering device. *Comput. Electron. Agr.* **2023**, *211*, 107997. [[CrossRef](#)]
20. Karayel, D.; Barut, Z.B.; Özmerzi, A. Mathematical modelling of vacuum pressure on a precision seeder. *Biosyst. Eng.* **2004**, *87*, 437–444. [[CrossRef](#)]
21. Singh, R.; Singh, G.; Saraswat, D. Optimisation of design and operational parameters of a pneumatic seed metering device for planting cottonseeds. *Biosyst. Eng.* **2005**, *93*, 429–438. [[CrossRef](#)]
22. Yazgi, A.; Degirmencioglu, A. Measurement of seed spacing uniformity performance of a precision metering unit as function of the number of holes on vacuum plate. *Measurement* **2014**, *56*, 128–135. [[CrossRef](#)]
23. Pareek, C.M.; Tewari, V.K.; Machavaram, R. Multi-objective optimization of seeding performance of a pneumatic precision seed metering device using integrated ANN-MOPSO approach. *Eng. Appl. Artif. Intel.* **2023**, *117*, 105559. [[CrossRef](#)]
24. Yu, J.; Liao, Y.; Cong, J.; Yang, S.; Liao, Q. Simulation analysis and match experiment on negative and positive pressures of pneumatic precision metering device for rapeseed. *Int. J. Agric. Biol. Eng.* **2014**, *7*, 1–12.
25. Han, D.; Zang, D.; Jing, H.; Yang, L.; Cui, T.; Ding, Y.; Wang, Z.; Wang, Y.; Zhang, T. DEM-CFD coupling simulation and optimization of an inside-filling air-blowing maize precision seed-metering device. *Comput. Electron. Agric.* **2018**, *150*, 426–438. [[CrossRef](#)]
26. Tang, H.; Xu, F.; Xu, C.; Zhao, J.; Wang, Y. The influence of a seed drop tube of the inside-filling air-blowing precision seed-metering device on seeding quality. *Comput. Electron. Agric.* **2023**, *204*, 107555. [[CrossRef](#)]
27. Xu, J.; Hou, J.; Wu, W.; Han, C.; Wang, X.; Tang, T.; Sun, S. Key structure design and experiment of air-suction vegetable seed-metering device. *Agronomy* **2022**, *12*, 675. [[CrossRef](#)]
28. Xu, C.; Xu, F.; Tang, H.; Wang, J. Determination of characteristics and establishment of discrete element model for whole rice plant. *Agronomy* **2023**, *13*, 2098. [[CrossRef](#)]
29. Hu, M.; Xia, J.; Zhou, M.; Liu, Z.; Xie, D. Design and experiment of seed-cleaning mechanism for inside-filling pneumatic cotton precision. *Agriculture* **2022**, *12*, 1217. [[CrossRef](#)]
30. Xu, J.; Sun, S.; He, Z.; Wang, X.; Zeng, Z.; Li, J.; Wu, W. Design and optimisation of seed-metering plate of air-suction vegetable seed-metering device based on DEM-CFD. *Biosyst. Eng.* **2023**, *4426*, 277–300. [[CrossRef](#)]
31. Zhao, X.; Zhang, T.; Liu, F.; Li, N.; Li, J. Sunflower seed suction stability regulation and seeding performance experiments. *Agronomy* **2023**, *13*, 54. [[CrossRef](#)]
32. Liu, R.; Liu, Z.; Zhao, J.; Lu, Q.; Liu, L.; Li, Y. Optimization and experiment of a disturbance assisted seed filling high-speed vacuum seed-metering device based on DEM-CFD. *Agriculture* **2022**, *12*, 1304. [[CrossRef](#)]

Disclaimer/Publisher’s Note: The statements, opinions and data contained in all publications are solely those of the individual author(s) and contributor(s) and not of MDPI and/or the editor(s). MDPI and/or the editor(s) disclaim responsibility for any injury to people or property resulting from any ideas, methods, instructions or products referred to in the content.